

Optical emission spectroscopy of metal-halide lamps: Radially resolved atomic state distribution functions of Dy and Hg

Abstract. Absolute line intensity measurements are performed on a metal-halide lamp. Several transitions of atomic and ionic Dy, and atomic Hg are measured at different radial positions from which we obtain absolute atomic and ionic Dy intensity profiles. From these profiles we construct the radially resolved Atomic State Distribution Function (ASDF) of the atomic and ionic Dy and atomic Hg. From these ASDFs several quantities are determined as a function of radial position, such as the (excitation) temperature, the ion ratio Hg^+/Dy^+ , the electron density, the ground state and total density of Dy atoms and ions. Moreover, these ASDFs give us insight about the departure from equilibrium. The measurements show a hollow density profile for the atoms and ionization of atoms in the centre. In the outer parts of the lamp molecules dominate.

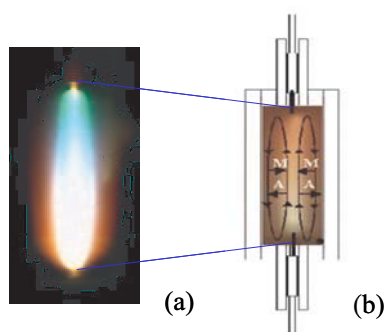


Figure 2.1: (a) Colour separation in a metal-halide lamp burner. (b) Schematic view of a metal-halide lamp; diffusion and convection of atoms (A) and molecules (M) are indicated by arrows. See figure 1.1 for full colour.

2.1 Introduction

The search for a compact high-intensity light source with high luminous efficacy and good colour rendering properties has led to the development of the metal-halide lamp [1]. This type of lamp contains a buffer gas of Hg and a relatively small amount of a mixture of additives such as Dy, Ce or Na salts, these act as the prime radiators. More than two salt components are necessary for a good color rendering index, therefore mixtures such as (NaI + ScI₃), (NaI + TlI + InI) or (NaI + TlI + DyI₃ + HoI₃ + TmI₃) are commonly used in the metal-halide lamp. Because of radial diffusion and convection these additives are non-uniformly distributed over the lamp resulting in the undesirable segregation of colours [2], see figure 2.1. In this study a lamp with an Hg buffer gas and one salt, namely DyI₃, is used. This lamp has a relatively simple salt system and therefore the results are easier to compare with a numerical model. Transport phenomena in this chemically complex plasma are not yet fully understood.

The aim of this work is to improve understanding of the plasma properties and transport phenomena in this type of lamps. The lamp is investigated using absolute line intensity measurements. The intensity of the lines are calibrated using a ribbon lamp with known spectral radiance. The spectrum of Dy contains a large abundance of lines, see figure 2.2, making wavelength calibration a complicated task. After intensity and wavelength calibration, these measurements yield absolute radial density distributions of several excited states of the additive Dy and the buffer gas Hg. From these the atomic state distribution functions (ASDF) are constructed for atomic and ionic Dy; and atomic Hg. From the ASDF several plasma properties can be determined such as the temperature, the ground state densities and the electron density. Moreover, the results may give an indication of a departure from equilibrium. This could be induced, for example, by transport phenomena such as segregation.

The few milligrams of the DyI₃ additive do not entirely evaporate leaving a liquid salt pool at the coldest spot of the burner wall. The cold spot determines the vapour pressure

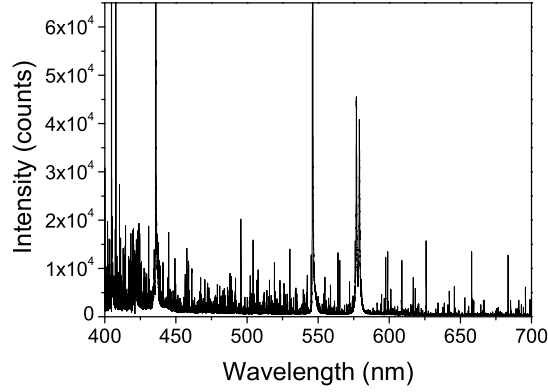


Figure 2.2: Spectrum of a metal-halide lamp containing Hg as a buffer gas and the additive DyI_3 . The saturated lines are Hg.

of the additive in the immediate vicinity of the salt pool. Because of the large temperature gradient between the wall (~ 1200 K) and the centre of the burner (~ 6000 K) [3] a multi-step process of dissociation of DyI_3 molecules towards the centre and association of atoms into molecules near the wall takes place. The reaction chain can be described as follows, increasing with temperature to the right,



At the hot center Dy atoms ionize and Dy ions are created,



Two mechanisms influence the distribution of particles in the plasma. First, there is a high temperature in the centre rapidly decreasing toward the wall, because of $p = nkT$, this results in a hollow profile of the mass distribution over the lamp. Second, there is the difference between the diffusion velocities of the atoms and molecules. The smaller and lighter Dy atoms diffuse faster than the larger and heavier molecules (DyI , DyI_2 , DyI_3). This difference in diffusion velocity results, in a steady-state, in an even more hollow profile of the elemental density of Dy; this is called radial segregation. Elemental density includes contributions from all molecular, atomic and ionic species of a particular element.

Convection in the lamp causes the hot gas to move upwards in the centre of the arc and downwards along the cool wall. This movement drags the high concentration of Dy near the wall downwards resulting in a high density of elemental Dy in the bottom of the arc. This is called axial segregation [2]. The combination of axial and radial segregation is shown in figure 2.1(b).

This chapter is organized as follows, section 2.2 deals with the theory of the atomic state distribution function and the absolute line intensity. Section 2.3 deals with the lamp

and the experimental setup used for the optical emission spectroscopy measurements. In section 2.4 the atomic state distribution function for different radial positions and its derived quantities are presented and discussed. It includes the radial density profiles of Dy atoms, ions and Hg atoms, and the radial profiles of electron density and temperature. We also study the effects of the large presence of Hg on the plasma.

Results of this work will aid the validation of the numerical models meant to simulate transport phenomena in metal-halide lamps.

2.2 Theory

2.2.1 The atomic state distribution function

A plasma region is said to be in Local Thermal Equilibrium (LTE) when, at a certain specific location, all the material particles are in equilibrium with each other. This means that for any collisional reaction the number of forward processes equals that of the corresponding backward processes [4]. However, photons can in principle escape from a plasma region in LTE, therefore emission is not necessarily compensated by the inverse process of absorption. By measuring the intensity of light-emitting atoms and ions, the density of these species can be determined, in case of optically thin lines. When in LTE, the atomic state distribution functions (ASDF) can be constructed from the density, these obey the distribution function as described by Boltzmann and Saha [4].

Another aspect of LTE is that the kinetic temperature of the electrons is the same as that of the heavy particles, i.e. $T=T_e = T_h$.

Figure 2.3 gives a sketch of the ASDF in LTE of two subsequent systems. Such a graph is expected for the atomic state distribution function (ASDF) of the atomic and ionic system of the additive in the lamp. It can be expressed by the Saha equation [5]

$$\eta_p = \eta_e \eta_r^+ \left(\frac{h^2}{2\pi m_e k T} \right)^{3/2} \exp(I_{pr}/k_B T), \quad (2.3)$$

where m_e , k , T_e , are the mass of the electron, the Boltzmann constant and the electron temperature respectively. I_{pr} is the energy difference between the atomic level p and ionic level r . In case of $r = 1$, which is the ground level of the ionic system, we have $I_{p1} \equiv I_p$, where I_p is the ionization energy. η_p is the corresponding state density defined as $\eta = n/g$, the number density n of an atom in a level p divided by the statistical weight g of that level. In the same way we can define $\eta_r^+ = n_r^+/g_r^+$, the state density of the ion and the state density of the free electron $\eta_e = n_e/g_e$ where $g_e = 2$, the number of the spin states of the free electron. When we use the Saha equation to find the relation between the atomic and the ionic ground state in Dy we need to insert the ionization potential of atomic Dy which equals $I_p = 5.93$ eV.

Two atomic levels that are in Saha relation with the ionic ground state are related to each other by Boltzmann's law, see figure 2.3. This can be understood by applying the

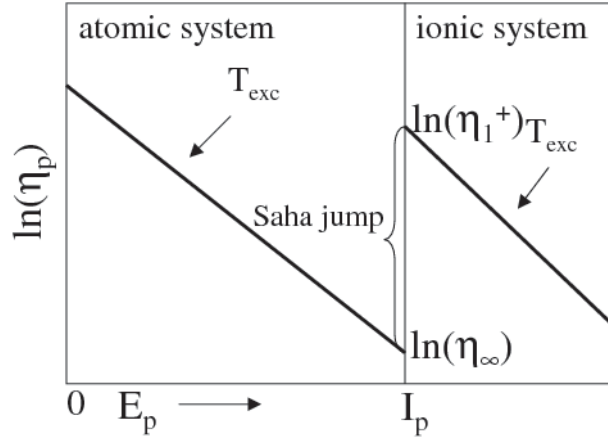


Figure 2.3: The ASDF of two subsequent atomic stages of one element (e.g. Dy) for a plasma in LTE. At the transition from the atomic to the ionic system the state density η shows a discontinuity. This is the so-called Saha jump and depends on the electron temperature and density, see equation 2.6. Note that there are two ways to indicate the energy position of an atomic level ‘p’, the excitation energy E_{1p} and the ionization potential I_{pr} . Going to the left along the energy axis I_{pr} will increase whereas E_{1p} decreases. [5]

Saha relation to two levels p and q and dividing the obtained expressions. This gives

$$\eta_q = \eta_p \exp(-E_{pq}/k_B T), \quad (2.4)$$

where $E_{pq} = I_p - I_q$, see figure 2.3. When the whole ASDF is consistent with Saha (and thus Boltzmann), the plasma region is said to be in Local Thermal Equilibrium [5].

We study the various features of the ASDF as shown in figure 2.3 with the aim to deduce essential plasma properties from it. Since figure 2.3 is a semi-log plot it is instructive to take the logarithm of the corresponding equation i.e. the Saha equation (2.3) which gives

$$\ln \eta_p = \frac{I_p}{k_B T} + \ln(\eta_\infty), \quad (2.5)$$

where

$$\eta_\infty = \eta_e \eta_1^+ \left(\frac{h^2}{2\pi m_e k_B T} \right)^{3/2}. \quad (2.6)$$

This near-continuum value of the atomic state density can be obtained by extrapolating η_p towards $I_p=0$. Other important densities are the atomic ground state density η_1 and the ionic ground state density η_1^+ . These can be obtained by extrapolating the ASDF towards $E_{1p}=0$ and $I_{p1}=0$ respectively.

The total ion density is found by taking the sum of all (excited) ions using the following expression:

$$n^+ = \sum_q n_q^+, \quad (2.7)$$

where

$$n_q^+ = \eta_1^+ g_q \exp\left(\frac{-E_q}{k_B T}\right), \quad (2.8)$$

where η_1^+ is the ionic ground state density. Rewriting equation 2.7 gives

$$n^+ = \eta_1^+ \sum_q g_q \exp\left(\frac{-E_q}{k_B T}\right) = \eta_1^+ Q(T). \quad (2.9)$$

$Q(T)$ is the partition function depending only on temperature and considered species [4]. The total atomic density of Dy can be calculated by means of the same expression in which the ionic ground state density is replaced by that of the atom and the partition function for the atom is used. In contrast to the Hg system, where we can replace the partition function by the g -value of the ground level ($g_1=2$) without loss of accuracy, the partition function must be taken into account for the Dy system. For instance the value for $Q(T)$ for Dy ions at $T = 5900\text{K}$ is 69 and for Dy atoms is 59 [12] whereas g_1 of Dy atoms and g_1 of Dy ions are 17 and 18 respectively.

We now introduce step-by-step how to extract information from the semi-log plot of figure 2.3.

1. The temperature value can be determined from the slope of the ASDF. This temperature can be indicated as the excitation temperature T_{exc} , which in LTE should be the same as the electron temperature T_e and heavy particle temperature T_h , see figure 2.3. Since we construct an ASDF for different species, namely Hg atoms, Dy atoms and ions, we will find T_{exc} values for each of these species. If the temperatures are equal to each other, within the estimated error margins, one of the necessary demands of the LTE assumption is satisfied.
2. By extrapolating the line in the atomic system toward the ground state (that is $E_{1p}=0$) we find the value of the atomic ground state density. As we can only measure the visible spectrum we cannot measure lines from low energy levels, therefore extrapolation is necessary.
3. By extrapolating the line in the atomic system toward the continuum (that is $I_p = 0$) we find the value of η_∞ . By extrapolating the line in the ionic system toward the continuum, we find the value of the ionic ground state η_1^+ , see figure 2.3.
4. The electron density n_e can be calculated from the Saha jump, which is the difference between the occupation of the highly excited state η_∞ and the ionic ground state η_1^+ . By determining η_∞ , η_1^+ (both by extrapolation) and T_e (from the slope), n_e can be calculated.

We recall that in a mixture, such as the composition of Hg and DyI_3 , the electrons present are supplied by both Hg and Dy, and are indistinguishable. Due to charge neutrality we may expect that the relation $n_e = n_i(\text{Hg}) + n_i(\text{Dy})$ holds. It will be shown that Hg is dominant in the lamp we studied.

The ionic ground state densities of Dy is determined with two different methods. One method ('Boltzmann method') calculates the ionic ground state density from the extrapolation of the ionic Dy lines in the Boltzmann plot to the ionization potential see equation 2.3. The other method ('Saha method') combines the value for η_∞ from the atomic Dy system with the electron density calculated using Hg (assuming $n_i = n_e$).

2.2.2 The absolute line intensity

In order to construct an ASDF we need to relate the intensity of Dy and Hg lines measured in the experiment to the absolute densities. If the plasma is optically thin, the radiation can escape the plasma as absorption can be neglected. The corresponding integrated emission coefficient of a particular transition j_{pq} [$\text{Wm}^{-3}\text{sr}^{-1}$], is defined as

$$j_{pq} = (1/4\pi)n_p A(p, q) E_{pq} \quad (2.10)$$

where n_p is the density of the upper level p, $A(p, q)$ the transition probability, $E_{pq} = E_{1p} - E_{1q} = h\nu_{pq}$, the energy of the emitted photon. This equation shows that the population density n_p of level p is proportional to the integrated emission coefficient j_{pq} ,

$$n_p = 4\pi \frac{j_{pq}}{A(p, q) E_{pq}} \quad (2.11)$$

The calibrated intensity I_{pq} [$\text{Wm}^{-2} \text{sr}^{-1}$] is determined by calibrating the line intensity of the metal-halide lamp with a tungsten ribbon lamp at the line of sight, over a plasma column of length D, and is given by

$$I_{pq} = \int_0^D j_{pq} ds. \quad (2.12)$$

j_{pq} is not necessarily constant over the length of the column, but could vary over the radial distance. Line intensities are measured at the line of sight. This means that the intensity of the spectral line is measured laterally, which is in our case along the horizontal cross-section of the burner. A lateral profile constitutes the integrated spectral line intensity as function of lateral position. Radial information can be extracted from a set of lateral measurements by the Abel inversion technique [7]. The radial intensity profile j_{pq} is approximated by means of a polynomial series [8],

$$j_{pq}(r) = a_0 + \sum_{n=2}^{\infty} a_n r^n. \quad (2.13)$$

The term $a_1 r$ is omitted because the derivative of the dysprosium density at the axis of the burner should be zero due to symmetry. Applying a least squares fitting procedure to the lateral profile the coefficients a_n are obtained and a radial profile is constructed.

After selecting a number of Dy and Hg lines from the measured spectrum of 400 to 800 nm, based on [9], the lateral profile of the corresponding emitting species can be

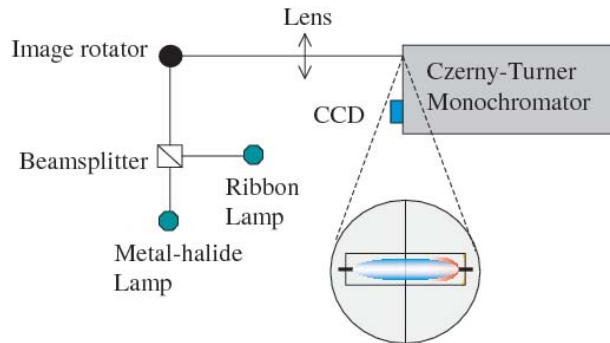


Figure 2.4: Setup consisting of a Czerny-Turner 1-meter monochromator, image rotator, beam splitter, and ST-2000 CCD camera. The CCD camera records the 2-D image of the light after being dispersed into different wavelengths by the grating of the monochromator. The wavelengths of the various atomic and ionic transitions are found on the horizontal scale. The image rotator optically rotates the image of the burner 90 degrees so it is projected horizontally onto the entrance slit, yielding a CCD image of the cross section of the burner on the vertical scale.

constructed. The radial profiles are then used to construct the ASDF for several radial positions. Measurements were done at different axial positions in the lamp, the results reported here were found at 3 mm above the bottom electrode with a $50 \mu\text{m}$ resolution in height.

2.3 Experimental setup

In the present experiment, emission spectroscopy is performed on a metal-halide lamp. The lamp consists of a quartz burner of 20 mm in length and 8 mm inner diameter and a transparent low-expansion quartz vacuum jacket. The burner is made of quartz in order to make the arc optically accessible. Because quartz does not withstand high temperatures, the chosen power is low, causing less of the additives to be present in the arc vapour than in commercially available lamps. The distance between the electrodes is approximately 18 mm. The lamp is dosed with 10.0 mg of Hg and 4.08 mg of DyI_3 . It is driven by a ballast with a 80 Hz square wave voltage, and operated with an average input power of 100 W.

The metal-halide lamp [6] is mounted on an optical rail in vertical position together with a beamsplitter, image rotator and a lens (focal length 200 mm), which focuses the lamp-image onto the entrance slit of the spectrometer, see figure 2.4. The Czerny-Turner 1-meter monochromator contains a 1200 lines per mm grating for wavelength separation and an ST-2000 CCD camera for 2-D imaging. This CCD chip is 1600 pixels wide and 1200 pixels high. The pixel size is $7.4 \mu\text{m}$ by $7.4 \mu\text{m}$. The image rotator rotates the lamp image 90° so that a horizontal cross-section of the lamp is imaged onto the vertical slit of the monochromator and then on the CCD camera. As the wavelength dispersion is in the horizontal direction we obtain, at one axial position, a complete lateral profile in one measurement. The two-

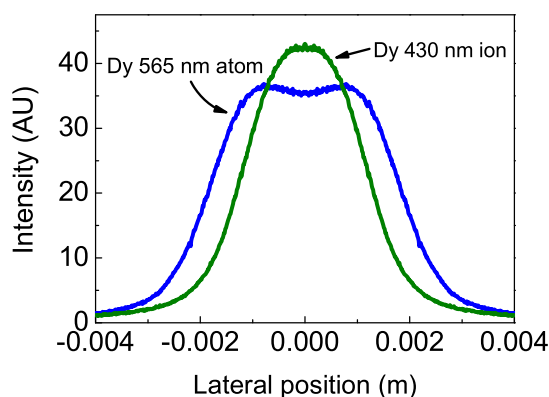


Figure 2.5: Lateral intensity profiles of atomic (at 565 nm) and ionic Dy (at 430 nm). The profiles are symmetrized with regard to the axis of the arc. The lines are measured 3 mm above the bottom electrode, the lamp power is 100 W.

dimensional CCD image therefore contains in the vertical direction the cross-section of the lamp and in horizontal direction the wavelengths of different atomic and ionic transitions. The intensity of the Dy and Hg lines are calibrated with a Tungsten ribbon lamp with known spectral intensity. The ribbon lamp is placed such that its calibrated light follows an optical path that is almost identical to that of the metal-halide lamp.

2.4 Results and discussion

Because the lateral profiles are not entirely symmetrical and cylinder symmetry is assumed, the lateral profiles are symmetrized with regard to the axis of the arc. The temperature at the axis is highest and the axis can therefore be found there where the intensity of Hg is highest. An example of the symmetrized lateral profiles in figure 2.5 shows the different lateral distributions of atomic and ionic species of Dy. Ions are at the centre, surrounded by atoms, which are in turn surrounded by (invisible) molecules near the wall. This is even more evident when looking at the radial intensity profiles in figure 2.6 derived from figure 2.5 using the previously described Abel inversion technique. There is a small dip in the centre of ionic Dy, this is most likely a temperature effect, as the temperature in the centre of the lamp is highest. It may also be caused by the Abel inversion technique, which is very sensitive for errors in the centre of the lateral profile.

From the radial profiles the ASDFs can be constructed for different radial positions. Figure 2.7 shows the ASDF at the axis of the lamp, 3 mm above the bottom electrode. Transition probabilities A from two different sources were used, Lawler [11] and Kurucz [9]. The measured lines and corresponding A values and relative errors are listed in the appendix.

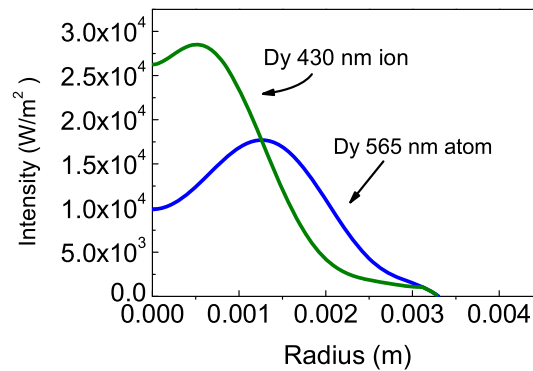


Figure 2.6: Calibrated radial intensity profiles of atomic (at 565 nm) and ionic Dy (at 430 nm). The lines are measured 3 mm above the bottom electrode, the lamp power is 100 W.

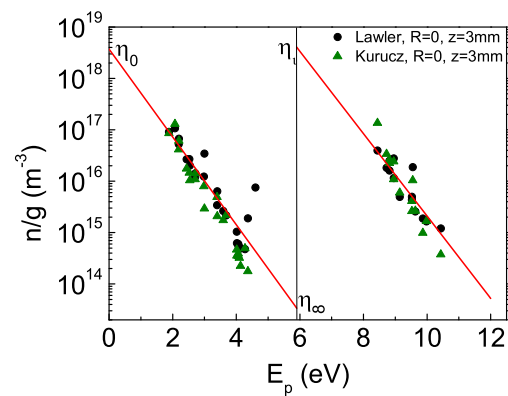


Figure 2.7: ASDF for Dy in the wavelength range of 400 to 700 nm. Emission lines are measured at the centre of the lamp 3 mm above the electrode. These results have been Abel inverted. The atomic and ionic transition probabilities are taken from Lawler [11] and Kurucz [9].

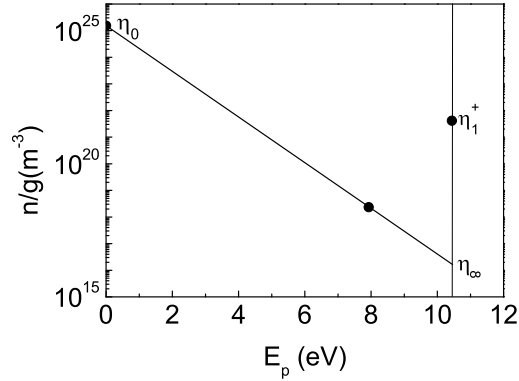


Figure 2.8: ASDF for Hg emission lines that are measured at the centre of the lamp 3 mm above the electrode. The ionization potential of Hg is at 10.44 eV. The ground state density is calculated from $p = nkT$. The intensity profile of the 407.8 nm line, with $A = 4 \cdot 10^6$ [11], at $E_p = 7.92$ eV has been Abel inverted.

The temperature for atomic Dy using the Lawler values is 5900 K and for ionic Dy it is 6300 K. The temperature for atomic Dy using the Kurucz values is 4700 K and for ionic Dy 4400 K. The Lawler values for A were found using an experimental technique that consists of a combination of fluorescent lifetime measurements of different levels and the determination of branching fractions by Fourier Transform Spectroscopy. The values of Kurucz were determined by estimation of the line intensity. Further results described in this paper make use of the Lawler values for A as we assume that the method used to determine them is more reliable. It is clear however that the errors in the A values are a strong limitation for the interpretation of our measurements. From the ASDF at different radial positions a radial temperature profile can be constructed for ionic and atomic Dy.

We now examine the Hg system. Only a small number of atomic Hg lines was observed, of which the energy levels were very close so that no accurate slope of the ASDF could be determined. This can be resolved by taking the absolute density of the ground state into account. First we calculate the ground state density of the Hg atom using the ideal gas law $p = nkT$. Due to the Hg dominance, n can be replaced by n_{Hg} density. As the pressure is constant over the lamp, nT is a constant over the whole plasma. We determine the pressure by calculating the total density of Hg inside the burner. This is done using the dimensions and Hg content of the lamp, which is 20 mm in height and 8 mm in diameter and contains 10 mg Hg, together with the assumption that the effective temperature equals 3000 K [10]. We then assume LTE and use the temperature profile for atomic Dy in combination with the calculated pressure to find the ground state density of Hg as function of the radius. It must be stated that the initial choice of temperature has limited effect on the results. In order to construct the ASDF we determine the absolute density at one line, at 407.8 nm, see figure 2.8. We can now calculate the temperature as a function of the radius.

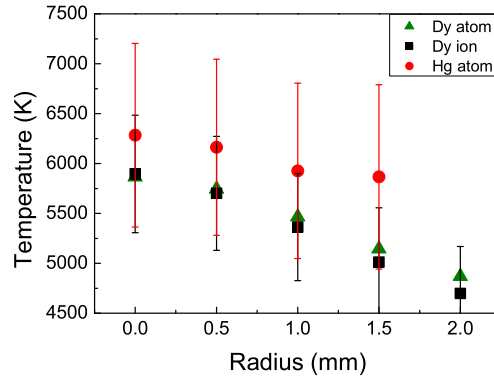


Figure 2.9: Temperature profiles for different radial positions, 3 mm above the bottom electrode. The lamp power is 100 W. The transition probabilities were taken from Lawler [11].

Figure 2.9 shows that the temperature profiles for atomic and ionic Dy and Hg are similar when taking the error of the linear fit of the scattered data points into account which, due to large scatter of the data points, is relatively high and about 10 to 14 percent.

Now that the temperature is known we calculate the ground states of atoms and ions as well as the electron density, and the total atomic and ionic density of Dy. From figure 2.7 and figure 2.8 it can be deduced that Hg is the dominant ion. Therefore the ratio between the Hg ion and the Dy ion has been calculated from these measurements. The ratio of Hg^+/Dy^+ ions is shown as function of the radius in figure 2.10, proving that Hg ions dominate over the Dy ions up to $R = 1.7$ mm. Because Hg ions are the leading system in the centre of the lamp, the bulk of the electrons are supplied by Hg. The electron density n_e was determined by calculating η_∞ by means of extrapolation of the atomic Hg ASDF and assuming $n_i = n_e$ for the inner region. The results are shown in figure 2.11.

Total atomic and ionic densities are also shown in figure 2.11. Dy atoms ionize into Dy ions in the hot centre of the lamp, causing a depletion of Dy atoms. The atomic density decreases toward the cooler wall making room for molecules. The atomic ground state density found by extrapolating the atomic ASDF is of the order $n_1 = 10^{20} \text{m}^{-3}$ (taking $g_1=17$). Flikweert *et al* [8] measured the atomic ground state density at different powers (at 113W and 151W), by means of laser absorption spectroscopy of a lamp of the same type. It was found that the value for the atomic ground state rapidly increases as function of power. An extrapolation to 100 W from these results leads to a similar value for the atomic ground state density.

The ratio between the ‘Saha method’ and the ‘Boltzmann method’ is depicted in figure 2.12. It shows that when moving away from the centre we see an increasing discrepancy between the two extrapolated ionic ground state densities. The ionic system is underpopulated with respect to the atomic system. This is what we expect as the ionic system suffers more loss of radiation than the atomic. This means that the Boltzmann balance of

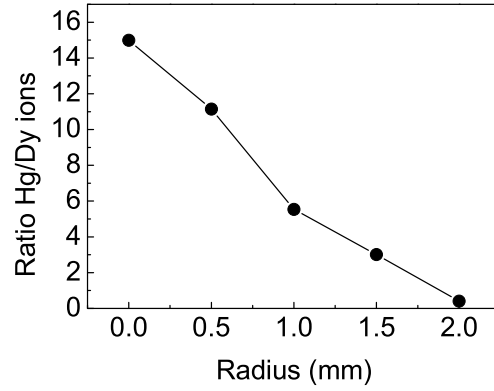


Figure 2.10: The ratio of Hg^+/Dy^+ ions for different radial positions. The total ionic density n^+ is calculated by combining the expression for η_∞ (equation 2.6) with the expression for n^+ (equation 2.9). η_∞ is found by means of extrapolation of the ASDF of Dy and Hg at different radial positions.

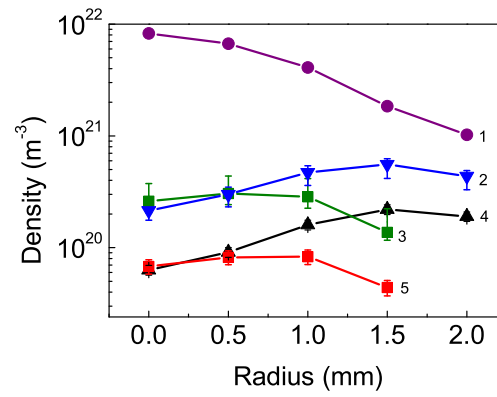


Figure 2.11: (1) electron density determined from the Hg ASDF. Total atomic (2) and ionic densities (3) for Dy. Atomic (4) and ionic (5) ground state densities for Dy.

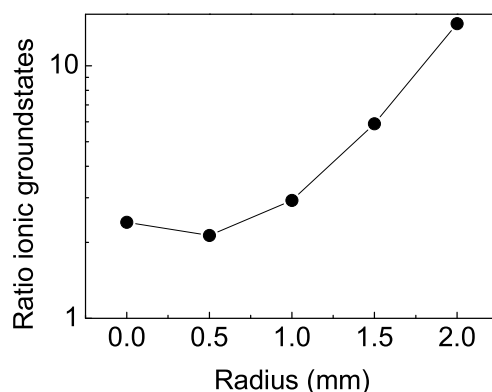


Figure 2.12: The ratio between the ionic ground state density calculated using the value for η_∞ , combined with the electron density calculated using the Hg density (assuming $n_i = n_e$); and the ionic ground state density calculated from the extrapolation of the ASDF for the Dy ion.

excitation and de-excitation is no longer in equilibrium and the assumption of LTE is no longer valid.

2.5 Conclusions

A radially resolved ASDF has been constructed for Dy and Hg for the metal-halide lamp. Radial intensity profiles of Dy show a clear separation between atomic and ionic regions in the plasma, the ionic region is in the hot centre, the atomic region surrounds it. The radial temperature profile constructed from the ASDF of atomic Dy shows a temperature of 5900 K in the centre of the lamp. The ionic and atomic temperature profile for Dy and the atomic Hg temperature profile are all equal within the error margins. Error margins are about 10 percent due to the large scatter in the data points, this can be remedied with better A values.

In this lamp driven at 100 W, Hg ions predominate in the centre of the discharge and contribute largely to the total electron density of the discharge. At the centre of the lamp there seems to be LTE, toward the wall there is a deviation of LTE with respect to the population of the Dy ionic system.

Future studies should include the measurement of the density distributions at different axial positions.

2.6 Acknowledgements

This research is supported by Technologiestichting STW (project ETF. 6093) and COST (project 529).

2.7 Measured lines and corresponding A values

Table I contains the A values for atomic Dy lines and Table II contains the A values for ionic Dy lines. A values are listed from Lawler [11] and Kurucz [9].

line (nm)	A value Lawler ($\times 10^6 \text{ s}^{-1}$)	A value Kurucz ($\times 10^6 \text{ s}^{-1}$)
402.371	29.0 $\pm 5\%$	58.55
411.305	23.4 $\pm 5\%$	92.10
412.608	0.92 $\pm 5\%$	73.1
413.035	1.76 $\pm 5\%$	1.84
414.606	195.0 $\pm 5\%$	347.8
419.802	108.0 $\pm 5\%$	214
423.202	79.0 $\pm 5\%$	146.8
423.985	94.0 $\pm 5\%$	145
424.591	118.0 $\pm 5\%$	178.9
429.196	2.28 $\pm 5\%$	6.159
448.436	4.65 $\pm 6\%$	10.48
456.509	0.66 $\pm 5\%$	0.864
457.778	1.96 $\pm 5\%$	2.448
488.016	0.520 $\pm 5\%$	0.7924
488.808	4.97 $\pm 5\%$	6.098
502.212	1.27 $\pm 5\%$	1.504
504.264	6.9 $\pm 5\%$	6.065
507.067	4.59 $\pm 5\%$	6.303
507.767	0.41 $\pm 8\%$	0.621
563.950	0.49 $\pm 8\%$	0.6007
565.201	0.446 $\pm 5\%$	0.4491
598.856	0.561 $\pm 5\%$	0.4636
616.843	0.81 $\pm 5\%$	1.702
657.937	0.77 $\pm 10\%$	0.8212

Table 2.1: A values used for the calculation of the density of atomic Dy. A values and relative errors from Lawler are given in [11]. Values from Kurucz [9] are based on data provided by either Gorshkov *et al* [13], where the relative error is estimated to be less than 50%; or by Meggers *et al* [14] from which the A values are determined from the estimated intensity.

line (nm)	<i>A</i> value Lawler ($\times 10^6 \text{ s}^{-1}$)	<i>A</i> value Kurucz ($\times 10^6 \text{ s}^{-1}$)
395.039	25 $\pm 6\%$	53.90
397.856	49.9 $\pm 5\%$	68.91
399.669	16.3 $\pm 6\%$	18.51
400.045	25.4 $\pm 5\%$	23.63
403.633	1.73 $\pm 8\%$	3.563
407.312	12.1 $\pm 7\%$	20.09
411.134	2.84 $\pm 5\%$	2.983
412.463	7.2 $\pm 5\%$	11.77
414.310	8.1 $\pm 8\%$	9.82
425.633	0.79 $\pm 5\%$	0.9048
430.863	2.78 $\pm 5\%$	1.71
444.970	1.97 $\pm 5\%$	1.062
446.814	0.451 $\pm 5\%$	0.4441
495.735	1.38 $\pm 5\%$	0.4011

Table 2.2: *A* values used for the calculation of the density of ionic Dy. *A* values and relative errors from Lawler are given in [11]. Values from Kurucz [9] are based on data provided by either Gorshkov *et al* [13], where the relative error is estimated to be less than 50%; or by Meggers *et al* [14] from which the *A* values are determined from the estimated intensity.

Bibliography

- [1] Lister G G, Lawler J E, Lapatovich W P and Godyak V A 2004 *Rev. Mod. Phys.* **76**, 541
- [2] Fischer E (1976) *J. Appl. Phys.* **47**, 2954
- [3] Zhu X 2005 Ph.D. thesis *Active spectroscopy on HID lamps*, Eindhoven University of Technology
- [4] Mitchner M and Kruger Jr CH 1973 *Partially ionized gases*, 1st ed., John Wiley and Sons
- [5] Van der Mullen J A M 1990 *Phys. Rep.* **191** 109
- [6] Stoffels W W, Kroesen G M W, Groothuis C H J M, Flikweert A J, Nimalasuriya T, Van Kemenade M, Kemps P, Bax M, Van den Hout F H J, Van den Akker D, Schiffelers G, Beckers J, Dekkers E, Moerel J, Brinkgreve P, Haverlag M, Keijser R and Kuipers A 2005 *Proceedings of the XXVIIth International Conference on Phenomena in Ionised Gases Eindhoven (16-342), july 17-22, E.M. Van Veldhuizen, Eindhoven University of Technology*
- [7] Curry J J, Sakai M and Lawler J E 1998 *J. Appl. Phys.* **84**, 3066
- [8] Flikweert A J, Nimalasuriya T, Groothuis C H J M, Kroesen G M W, and Stoffels W W, 2005, *J. Appl. Phys.* **98** 073301
- [9] Kurucz R L and Bell B 1993 *Atomic Line Data CD-ROM No 23* (Cambridge, MA: Smithsonian Astrophysical Observatory)
- [10] Elenbaas W 1951 *The high pressure mercury vapour discharge*, 1st ed., (North-Holland publishing company)
- [11] Wickliffe M W and Lawler J E 2000 *J. Quant. Spectrosc. Radiat. Transfer* **66**, 363
- [12] http://www.thespectroscopynet.com/Theory/Partition_Functions.asp
- [13] Gorshkov V N, Komarovskii V A, Oserovich A L, Penkin N P and Khefferlin R 1980 *Opt. Spectrosk.* **48**, 657-661
- [14] Meggers W F, Corliss C H and Scribner B F 1975 *Tables of Spectral-line intensities Part 1-Arranged by elements*, 2nd ed., (National Bureau of Standards)